Synergy of synthesis, computation and NMR reveals correct baulamycin structure

Jingjing Wu,[1†] Paula Lorenzo,[1†] Siying Zhong,[1†] Muhammad Ali,[1] Craig P. Butts,[1]* Eddie L. Myers[1]* & Varinder K. Aggarwal[1]*

[1] School of Chemistry, University of Bristol, Cantock's Close, Bristol BS8 1TS, UK

[†] These authors contributed equally to this work

* Email: V.Aggarwal@bristol.ac.uk; Eddie.Myers@bristol.ac.uk; Craig.Butts@bristol.ac.uk

Small-molecule bioactive natural products continue to be our most rewarding source and inspiration for new medicines.[1] Sometimes we happen upon such molecules in minute quantities in unique, difficult-to-reach, and often fleeting environments, perhaps never to be rediscovered again. In these cases, structure determination, including the assignment of relative- and absolute configuration, is paramount. Molecules comprising stereochemically complex acyclic and conformationally flexible carbon chains make the task extremely challenging.[2] The baulamycins serve as a contemporary example. Isolated in small quantities and shown to have promising antibiotic activity, the structure of the conformationally flexible molecule was based largely on *J*-based configurational analysis,[3] but has been found to be incorrect.[4,5] Our subsequent campaign to identify the true structure of the baulamycins has revealed a powerful method for the rapid structural elucidation of such molecules. Specifically, DFT-led prediction of NMR parameters, combined with an efficient medley of boron-based synthetic transformations, which allowed an encoded mixture of natural product diastereomers to be prepared, enabled us to rapidly pinpoint and synthesise the correct structure.

Antimicrobial resistance poses an increasing global public health threat to society.[6,7] To address this problem, chemical agents that operate through novel modes of action, especially those that are unique to the offending microorganism, offer new opportunities.[8] For example, iron, which is essential for growth and survival of organisms, is carried into microbial cells with the aid of siderophores. Inhibiting the biosynthesis of siderophores provides a mechanism of action unique to the pathogen because mammalian host cells employ other mechanisms to regulate iron concentration.[9] From a library of 19,855 marine microbial-derived natural products, and using an assay to target siderophore biosynthesis, Sherman *et al.* identified two natural products, baulamycin A and B, which were active against the superbug MRSA and Bacillus anthracis (baulamycin A - 69 μM and 110 μM).[4,5] The limited availability of both baulamycin A and B (3.6 mg and 2.1 mg, respectively, were obtained from 39 L of culture), precluded chemical modification as a means to aid in structural assignment, which was thus guided entirely by isotropic solution-state NMR spectroscopy—principally, empirical *J*-based configurational analysis.[3]

Because biological study was similarly limited by supply of the natural products, we have targeted their syntheses. In this paper, we report a 10-step synthesis of the proposed structures of baulamycin A (**1**) and B (**2**), but unfortunately found that the data did not match that of the natural products. During the course of our work, Guchhait *et al.* reported a 17-step synthesis

of the proposed structure of baulamycin A.[10] They similarly found that the data did not match and further attempts to prepare the correct diastereomer based on re-examination of the *J*-based configurational analysis was also unsuccessful.

Elucidating the structures of natural products that are only available in very small quantities is often an exceptionally difficult task, highlighted by the high number of structure revisions reported every year in the chemical literature.[2] This challenge is epitomized in the baulamycins, which contain 7 stereogenic centres (128 possible stereoisomers), of which only 3 are contiguous, distributed along a 14-carbon-long chain. The flexibility of the chain leads to experimental NMR parameters that are a weighted average from an ensemble of conformations. This severely complicates configurational analysis to an extent where standard approaches based on empirical NMR analysis[3] or even recent quantum chemical approaches using chemical shift data[11–13] are insufficient. However, combining accurate quantum chemical prediction of the ensemble-averaged NMR parameters with the analysis of encoded stereoisomeric mixtures, which were accessible through the power of iterative reagent-controlled homologation of boronic esters (assembly-line synthesis),[14] have enabled us to correct five of the seven stereogenic centers and finally establish the correct structure of these important natural products.

Our retrosynthetic analysis of baulamycin A (**1**) and B (**2**) resulted in a disconnection at C11–C12, thus dividing the target molecule into equally complex halves, fragments A and B (Figure 1a). We considered their union through a late-stage lithiation–borylation reaction, a process utilising our recently reported regio- and stereoselective homologation of a 1,2-bis(boronic esters).[15] Fragment A could be obtained through a Morken hydroxy-directed diboration of homoallylic alcohol **6**,[16] which itself could be obtained by Antilla allylboration.[17,18] Fragment B was envisaged to come from our recently developed assembly-line synthesis,[14] a process that readily lends itself to the synthesis of analogues. We began with the synthesis of fragment A (Figure 1b). Rhodium-catalyzed hydroboration of alkyne **13** gave *Z*-vinyl boronic ester **14**,[19] which was homologated with chloromethyl lithium[20] to give *Z*-allyl boronic ester **8**. Antilla allylboration of the methoxymethyl(MOM)-protected aldehyde gave the homoallylic alcohol **16** in good yield, high diastereoselectivity, and high enantioselectivity.[17,18] Subsequent Morken hydroxy-directed diboration,[16] gave the 1,2-bis(boronic ester) (*R*,*S*,*R*)-**17** (after protection of the hydroxy group as the TES ether) in 98:2 d.r., thus completing a short highly stereoselective synthesis of fragment A. The synthesis of fragment B commenced with rhodium-catalyzed hydroboration of allyl benzoate **19** to give boronic ester **12**,[21,22] the starting material for assembly-line synthesis (Figure 1c). Then, sequential treatment of boronic ester **12** with the carbenoids (*S*)-**11**, chloromethyl lithium (**10**), (*R*)-**11**, **10** and finally (*S*)-**11**, gave the target boronic ester **9** in 64% yield. To complete fragment B, we decided to introduce an enol ether as a masked ketone, through a Zweifel olefination.[23] Thus, boronic ester **9** was treated with lithiated MOM vinyl ether **20** and the ethenyl variant **21**,[24] followed by treatment with I_2, giving the desired variants of fragment B, (*R*,*S*,*R*)-**22** and (*R*,*S*,*R*)-**23**, in 72 and 86% yield, respectively. Fragment union (Figure 1d) involved lithiation of the benzoate ester (**22** or **23**) followed by regioselective homologation of the primary boronic ester moiety of 1,2-bis(boronic ester) (*R*,*S*,*R*)-**17**,[15] to give the 1,3-bis(boronic ester), which after oxidation gave the desired diols **24** and **25** with high stereoselectivity (95:5 d.r.). Finally, treatment with aq. HCl in THF/MeOH effected removal of the silyl and MOM groups, completing a short synthesis of the proposed structures of baulamycin A (**1**) and B (**2**).[5]

Unfortunately, the ^{1}H- and ^{13}C NMR spectra of the synthetic samples did not match those of the reported natural products, leading us to conclude that one or more of the stereogenic centers of the natural products had been misassigned. But which of the seven stereogenic centres was incorrect? It was clearly not practical to make all 128 stereoisomers, so further analysis of the NMR data was required. The molecule can be divided into two halves and we initially considered fragment A, the C10–C1′ portion. Comparing the observed coupling constant for the vicinal protons of C1′–C14 in our synthetic material (3.6 Hz) to that of the natural product (7.2 Hz) we reassigned the *syn* configuration of C1′–C14 originally proposed for the natural product to *anti*. The small and large coupling constants are characteristic of *syn* and *anti* motifs, respectively, in similar fragments reported in the literature.[25-27] The NMR parameters for the C10–C1′ region of the four remaining diastereomers, **26**–**29**, which arise from varying the configuration at C13 and C11, were computed for comparison with the parameters of the isolated material. For this computational analysis, the relative stereochemical configuration in fragment B was maintained as *anti–anti*, as reported in the original paper.

Conformational analysis of diastereomers **26**–**29** using molecular mechanics found between 650 and 2455 conformations for each diastereomer. For each diastereomer, low-energy conformers (~84–196 conformers) were submitted to sequential DFT geometry optimization and free-energy calculations (Figure 2d). The populations of the resulting conformers were further refined based on the quantitative interproton distances[28] calculated from Sherman *et al.* ROESY measurements. The conformers predicted to make up >85% of the ensemble populations of diastereomers **26**–**29** (8–28 conformers) were subjected to DFT calculations for the prediction of coupling constants for the C10–C1′ regions. We then compared both the calculated ^{1}H–^{1}H coupling constants and the NOE-derived interproton distances for the C10–C1′ region of diastereomers **26**–**29** with the corresponding experimental data for the isolated natural product, baulamycin A, and applied a statistical analysis based on χ^2 (reduced) values (Figure 2c), where acceptable models must have values approaching 1. Based on ^{1}H–^{1}H coupling constants alone, there in an excellent fit for the C10–C1′ region of **29** ((χ^2 (reduced) = 1.5), moderate fits but potentially viable matches for both **26** (χ^2 (reduced) = 2.4) and **27** (χ^2 (reduced) = 2.1) and no reasonable fit possible for **28** (χ^2 (reduced) = 6.2). Based on NOE distances alone, there are good fits for **28** and **29** (χ^2 (reduced) = 1.4 and 1.7 respectively) and poor fits for **26** and **27** (χ^2 (reduced) = 5.3 and 5.4, respectively). Similarly, comparison of the DFT-predicted NMR parameters of the structure originally proposed for baulamycin A, **1**, with the experimental NMR data of the isolated material revealed that both sets of NMR parameters did not fit simultaneously (χ^2 (reduced) = 1.6 and 5.1 for ^{1}H–^{1}H coupling constants and NOE distances, respectively). Thus, diastereomer **29** was the only structure that fitted both experimental NMR parameters simultaneously for fragment A. The analysis had thus identified the relative configuration of four of the seven stereogenic centres, thus reducing the possible isomers of baulamycin from 128 down to 16. This assignment is also supported by χ^2 (reduced) analysis of computed chemical shifts and ^{1}H–^{13}C coupling constants, although neither was as discriminating as analysis based on ^{1}H–^{1}H coupling constants and NOE distances. Applying comparable analyses from Willoughby *et al.*[11] or the DP4 method of Goodman *et al.*,[12] based on computed NMR chemical shifts for diastereomers **1** and **26**–**29** could not alone provide structural discrimination, thus highlighting the care that must be taken with NMR-based stereochemical analysis of flexible complex molecules. The revised *anti–anti* fragment A, (***R***,***R***,***R***)-**34**, was synthesized by employing the same highly diastereoselective method used for

(***R***,***S***,***R***)-**17** but using the *E*-allyl boronic ester **32**[29] in place of the corresponding *Z* isomer in the Antilla allylboration (Figure 2e).

Computational analysis of fragment B (C4–C8) for diastereomers **29** and **35**–**37** was also undertaken, but in this case only ^{1}H–^{1}H coupling constants were computed (Figure 3c) owing to overlap in the critical region of Sherman *et al.*'s 2D ROESY spectrum. This analysis indicated that diastereomers **29** and **35** were very poor fits (χ^2(reduced) = 4.7 and 8.6, respectively) and could be excluded from consideration; however, *syn–anti* and *syn–syn* diastereomers **36** and **37** could not be discriminated (χ^2(reduced) = 1.6 and 1.6, respectively) based on ^{1}H–^{1}H coupling constants alone. Further analysis of the fits of chemical shifts, whilst less discriminating than fits of coupling constants, suggested that *syn–syn* diastereomer **37** gave a good fit (χ^2(reduced) = 0.2 and 0.6 for ^{1}H and ^{13}C chemical shifts, respectively) but *syn–anti* diastereomer **36** fitted less well (χ^2(reduced) = 0.9 and 2.9, respectively).

In parallel, we sought to determine the relative configuration of fragment B through synthesis. We anticipated that the most powerful aspect of assembly-line synthesis, that is, the exquisite reagent control over stereoselectivity, could be used to rapidly generate an encoded mixture of all four diastereomers of fragment B, the identity of each diastereomer being indicated by its relative population. The strategy is reminiscent of Curran's fluorous-mixture synthesis, which was used to rapidly identify stereoisomers of a given natural product.[30] Specifically, growing the C11–C1 carbon chain by using chiral carbenoids with moderate, yet accurately measured e.r. values (for C8, C6 and C4) would lead to fragment B as a mixture of all four diastereomers, where the relative population of each diastereomer could be accurately predicted (Figure 3d). Linking the revised *anti–anti* fragment A with this diastereomeric mixture would give a mixture of diastereomers **29** and **35**−**37**. Comparison of the resulting ^{13}C NMR spectrum with that of the isolated material and noting the relative integration of the matching peaks should immediately confirm the relative configuration of the methyl-group-rich region. At this stage, we decided to prepare only one enantiomeric series of the four diastereomers of fragment B. We would then resolve, at a later stage, the remaining stereochemical elements.

For this approach, we needed to ensure that the relative populations of diastereomers was such that all four diastereomers could be accurately quantified by NMR spectroscopy and that they were maximally distributed in terms of peak intensity. We therefore selected e.r. values (*S*:*R*) of >99.9:0.1, 72:28 and 64:36 for α-stannyl ethyl benzoate, the carbenoid precursor to be used in the assembly-line synthesis, at the 1st (C8), 3rd (C6), and 5th (C4) iterations, respectively. These e.r. values were calculated to lead to a 46:26:18:10 mixture of diastereomers **37**/**36**/**29**/**35**. Using *R*/*S* mixtures of carbenoid precursors with accurately measured e.r. values, we obtained fragment B as a 47:25:18:10 mixture of diastereomers (Figure 3d). The almost perfect match between the expected and observed ratio of diastereomers showed that the homologation reactions operated under full reagent control. The mixture was carried forward for fragment coupling and removal of protecting groups (Figure 3d) to give the desired mixture of baulamycin A diastereomers, the 47:25:18:10 ratio being retained with high fidelity. Comparison of the ^{13}C NMR spectrum of the mixture of diastereomers (Figure 3e) with that of the isolated natural product revealed that the chemical shifts of the diastereomer with the highest population matched those of the natural product closely and, in agreement with the DFT calculations, this established that the correct relative configuration of fragment B was indeed *syn–syn*, not *anti–anti* as originally proposed.

With relative configuration within each fragment established, we set out to determine which of the two remaining diastereomers (C11/C8 *syn* or C11/C8 *anti*) was baulamycin A (Figure 4). The two enantiomers of the *anti–anti–syn* diastereomer of fragment A [(***R***,***R***,***R***)-**34** and (***S***,***S***,***S***)-**38**] were coupled to the *syn–syn* diastereomer of fragment B [(***R***,***R***,***R***)-**39**]. As expected, the two diastereomers, **37** and **40**, had almost identical ^{13}C NMR spectra, but very small differences at C7, C9, and C11 were discernable, with the C11/C8 *syn* diastereomer matching the natural product perfectly. Furthermore, the diastereomers exhibited marked differences in certain regions of the ^{1}H NMR spectra, the C11/C8 *syn* diastereomer **37** again matching the spectrum of the natural product perfectly. However, the optical rotation of the synthesized matching diastereomer **37** was positive whereas that of the isolated natural product was negative, thus indicating that compound **37** was the enantiomer of the natural product. To prepare the correct enantiomer of baulamycin A, fragment A (***S***,***S***,***S***)-**38** and fragments B (***S***,***S***,***S***)-**41** were linked together to ultimately give baulamycin A. Baulamycin B, with the revised configuration, was also synthesized using the same protocol, the analytical data fully matching that of the reported natural product.

References

(1) Newman, D. J. & Cragg, G. M. Natural Products as Sources of New Drugs from 1981 to 2014. *J. Nat. Prod*. **79**, 629–661 (2016).

(2) Nicolaou, K. C. & Snyder, S. A. Chasing molecules that were never there: misassigned natural products and the role of chemical synthesis in modern structure elucidation. *Angew. Chem. Int. Ed. Engl*. **44**, 1012–1044 (2005).

(3) Matsumori, N., Kaneno, D., Murata, M., Nakamura, H. & Tachibana, K. Stereochemical determination of acyclic structures based on carbon−proton spin-coupling constants. A method of configuration analysis for natural products. *J. Org. Chem*. **64**, 866–876 (1999).

(4) Tripathi, A., Schofield, M. M., Chlipala, G. E., Schultz, P. J., Yim, I., Newmister, S. A., Nusca, T. D., Scaglione, J. B., Hanna, P. C., Tamayo-Castillo, G. & Sherman, D. H. Baulamycins A and B, broad-spectrum antibiotics identified as inhibitors of siderophore biosynthesis in Staphylococcus aureus and Bacillus anthracis. *J. Am. Chem. Soc*. **136**, 1579–1586 (2014).

(5) Tripathi, A., Schofield, M. M., Chlipala, G. E., Schultz, P. J., Yim, I., Newmister, S. A., Nusca, T. D., Scaglione, J. B., Hanna, P. C., Tamayo-Castillo, G. & Sherman, D. H. Correction to "Baulamycins A and B, broad-spectrum antibiotics identified as inhibitors of siderophore biosynthesis in Staphylococcus aureus and Bacillus anthracis". *J. Am. Chem. Soc*. **136**, 10541–1541 (2014).

(6) O'Neill, J. Antimicrobial resistance: tackling a crisis for the health and wealth of nations. *Rev. Antimicrob. Resist*. (2014).

(7) WHO. Antimicrobial resistance: global report on surveillance. (WHO, Geneva, 2014).

(8) Fischbach, M. A. & Walsh, C. T. Antibiotics for emerging pathogens. *Science* **325**, 1089–1093 (2009).

(9) Quadri, L. E. N. Strategic paradigm shifts in the antimicrobial drug discovery process of the 21st century. *Infect. Disord. Drug Targets* **7**, 230–237 (2007).

(10) Guchhait, S., Chatterjee, S., Ampapathi, R. S. & Goswami, R. K. Total synthesis of reported structure of baulamycin A and its Congeners. *J. Org. Chem*. **82**, 2414–2435 (2017).

(11) Willoughby, P. H., Jansma, M. J. & Hoye, T. R. A guide to small-molecule structure assignment through computation of (1H and 13C) NMR chemical shifts. *Nature Protocols* **9**, 643–660 (2014).
(12) Smith, S. G. & Goodman, J. M. Assigning stereochemistry to single diastereoisomers by GIAO NMR calculation: the DP4 probability. *J. Am. Chem. Soc*. **132**, 12946–12959 (2010).
(13) Lodewyk, M. W., Siebert, M. R. & Tantillo, D. J. Computational prediction of ^{1}H and ^{13}C chemical Shifts: a useful tool for natural product, mechanistic, and synthetic organic chemistry. *Chem. Rev*. **112**, 1839–1862 (2012).
(14) Burns, M., Essafi, S., Bame, J. R., Bull, S. P., Webster, M. P., Balieu, S., Dale, J. W., Butts, C. P., Harvey, J. N. & Aggarwal V. K. Assembly-line synthesis of organic molecules with tailored shapes. *Nature* **513**, 183–188 (2014).
(15) Fawcett, A., Nitsch, D., Ali, M., Bateman, J. M., Myers, E. L. & Aggarwal, V. K. Regio- and stereoselective homologation of 1,2-bis(boronic esters): stereocontrolled synthesis of 1,3-diols and Sch 725674. *Angew. Chem. Int. Ed. Engl*. **55**, 14663–14667 (2016).
(16) Blaisdell, T. P., Caya,T. C., Zhang, L., Sanz-Marco, A. & Morken, J. P. Hydroxyl-directed stereoselective diboration of alkenes. *J. Am. Chem. Soc*. **136**, 9264–9267 (2014).
(17) Jain, P. & Antilla, J. C. Chiral Brønsted acid-catalyzed allylboration of aldehydes. *J. Am. Chem. Soc*. **132**, 11884–11886 (2010).
(18) Grayson, M. N., Pellegrinet, S. C. & Goodman, J. M. Mechanistic insights into the BINOL-derived phosphoric acid-catalyzed asymmetric allylboration of aldehydes. *J. Am. Chem. Soc*. **134**, 2716–2722 (2012).
(19) Ohmura, T., Yamamoto, Y. & Miyaura, N. Rhodium- or iridium-catalyzed trans-hydroboration of terminal alkynes, giving (Z)-1-alkenylboron compounds. *J. Am. Chem. Soc*. **122**, 4990–4991 (2000).
(20) Sadhu, K. M. & Matteson, D. S. (Chloromethyl)lithium: Efficient generation and capture by boronic esters and a simple preparation of diisopropyl (chloromethyl)boronate. *Organometallics* **4**, 1687–1689 (1985).
(21) Molander, G. A., Yun, C. S., Ribagorda, M. & Biolatto, B. B-alkyl Suzuki-Miyaura cross-coupling reactions with air-stable potassium alkyltrifluoroborates. *J. Org. Chem*. **68**, 5534–5539 (2003).
(22) Pereira, S. & Srebnik, M. Transition metal-catalyzed hydroboration of and CCl_4 addition to alkenes. *J. Am. Chem. Soc*. *118*, 909–910 (1996).
(23) Zweifel, G., Arzoumanian, H. & Whitney, C. C. A convenient stereoselective synthesis of substituted alkenes via hydroboration-iodination of alkynes. *J. Am. Chem. Soc*. **89**, 3652–3653 (1967).
(24) Tamao, K., Nakagawa, Y. & Ito, Y. *Org. Synth*. **73**, 94 (1996).
(25) Rohr, K., Herre, R. & Mahrwald, R. Toward asymmetric aldol-tishchenko reactions with enolizable aldehydes: access to defined configured stereotriads, tetrads, and stereopentads. *J. Org. Chem*. **74**, 3744–3749 (2009).
(26) Sellars, J. D. & Steel, P. G. Application of silacyclic allylsilanes to the synthesis of b-hydroxy-d-lactones: synthesis of Prelactone B. *Tetrahedron* **65**, 5588–5595 (2009).
(27) Ruiz, J., Karre, N., Roisnel, T., Chandrasekhar, S. & Grée, R. From protected β-hydroxy acylsil-anes to functionalized silyl enol ethers and applications in Mukaiyama aldol reactions. *Eur. J. Org. Chem*. 773–779 (2016).

(28) Jones C. R., Greenhalgh M. D., Bame J. R., Simpson T. J., Cox R. J., Marshall J. W. and Butts C. P. Subtle temperature-induced changes in small molecule conformer dynamics – observed and quantified by NOE spectroscopy *Chem. Commun.,* **52**, 2920-2923 (2016).
(29) Dutheuil, G., Selander, N., Szabó, K. J. & Aggarwal, V. K. Direct synthesis of functionalized allylic boronic esters from allylic alcohols and inexpensive reagents and catalysts. *Synthesis* 2293–2297 (2008).
(30) Curran, D. P., Sinha, M. K., Zhang, K., Sabatini, J. J. & Cho, D–H. Binary fluorous tagging enables the synthesis and separation of a 16-stereoisomer library of macrosphelides. *Nature Chem*. **4**, 124–129 (2012).

Additional information

Supplementary information and chemical compound information are available in the online version of the paper.

Acknowledgements

We thank EPSRC (EP/I038071/1) and the European Research Council (FP7, ERC grant no. 670668) for financial support and BBSRC/ EPSRC-funded BrisSynBio Research Centre (L01386X) for providing the 700MHz NMR spectrometer used. Parts of this work were carried out using the computational facilities of the Advanced Computing Research Centre, University of Bristol - http://www.bris.ac.uk/acrc/. P.L. thanks Xunta de Galicia, M.A. thanks HEC Pakistan and J.W. thanks the Shanghai Institute of Organic Chemistry for Postdoctoral Fellowships. S.Z. thanks the EPSRC Bristol Chemical Synthesis Doctoral Training Centre for a studentship (EP/L015366/1). We thank David Sherman for providing the raw NMR (FID) data of baulamycin A.

Author Contributions

V.K.A., E.L.M. and C.P.B. designed and lead the project. P.L., J.W. and M.A. conducted and designed the synthesis experiments and analysed the data. S.Z. performed computational and NMR studies and analysed the data. All authors contributed to the writing of the manuscript.

Author Information

Reprints and permissions information is available at www.nature.com/reprints. The authors declare no competing financial interests. Correspondence and requests for materials should be addressed to V.K.A., (v.aggarwal@bristol.ac.uk), E.L.M. (eddie.myers@bristol.ac.uk) or C.P.B. (Craig.Butts@bristol.ac.uk).

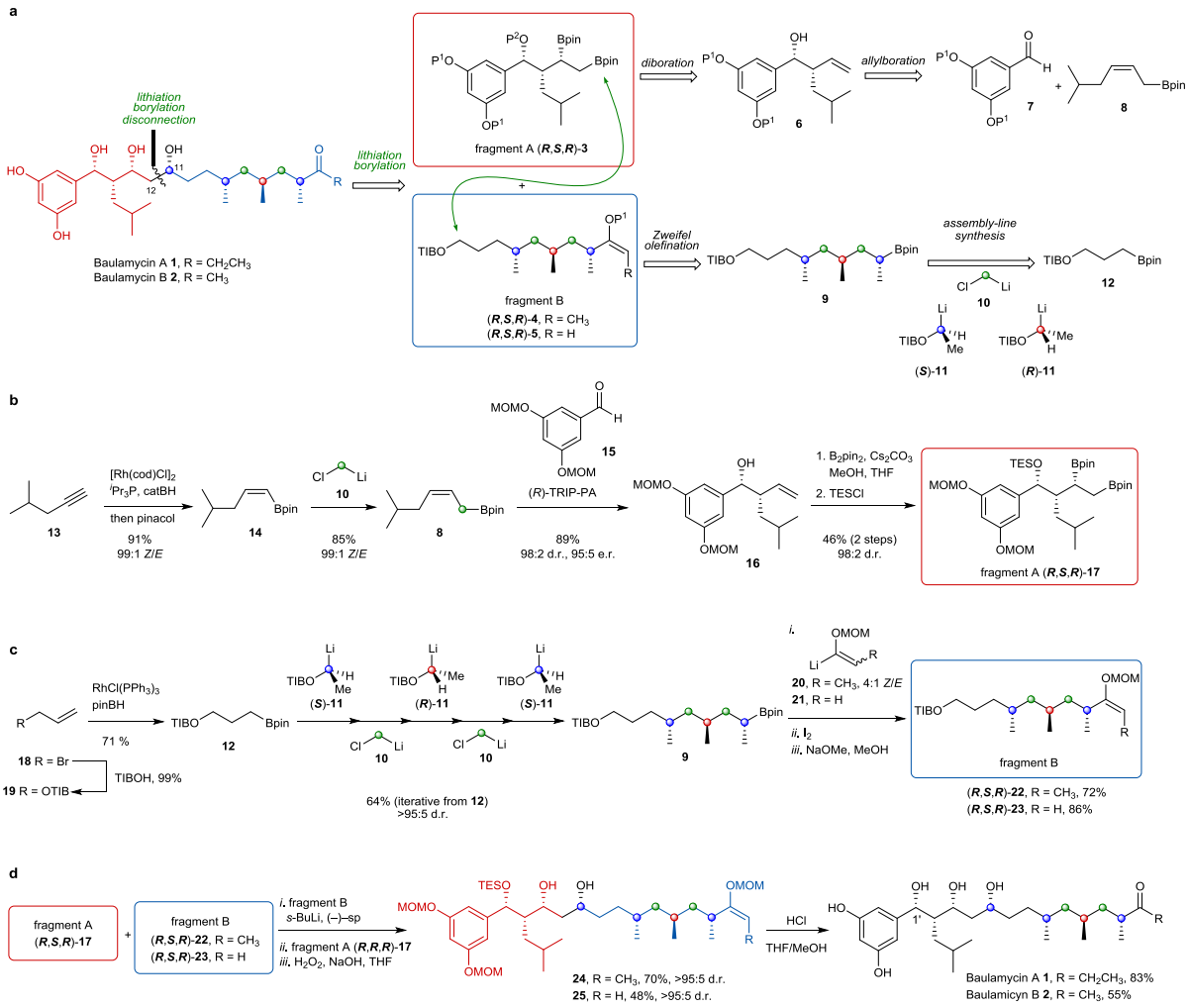

Figure 1. Retrosynthetic analysis and synthesis of originally proposed structure of baulamycin A and B. a, Disconnection across the C11–C12 bond gives two fragments, which can be combined using a late-stage lithiation–borylation reaction. Fragments A and B can be assembled from smaller building blocks. P, protecting group; TIB, 2,4,6-triisopropylbenzoyl; pin, pinacolato. **b**, Synthesis of fragment A (***R***,***S***,***R***)-**17**. **c**, Synthesis of fragment B, (***R***,***S***,***R***)-**22** and (***R***,***S***,***R***)-**23**, for baulamycin A and B, respectively. **d**, Fragment union and deprotection to give proposed structures for baulamycin A (**1**) and B (**2**). cat, catecholato; cod, cyclooctadiene; TRIP-PA, 3,3′-bis(2,4,6-triisopropylphenyl)-1,1′-binaphthyl-2,2′-diyl hydrogenphosphate; MOM, methoxymethyl; TES, triethylsilyl; sp, sparteine.

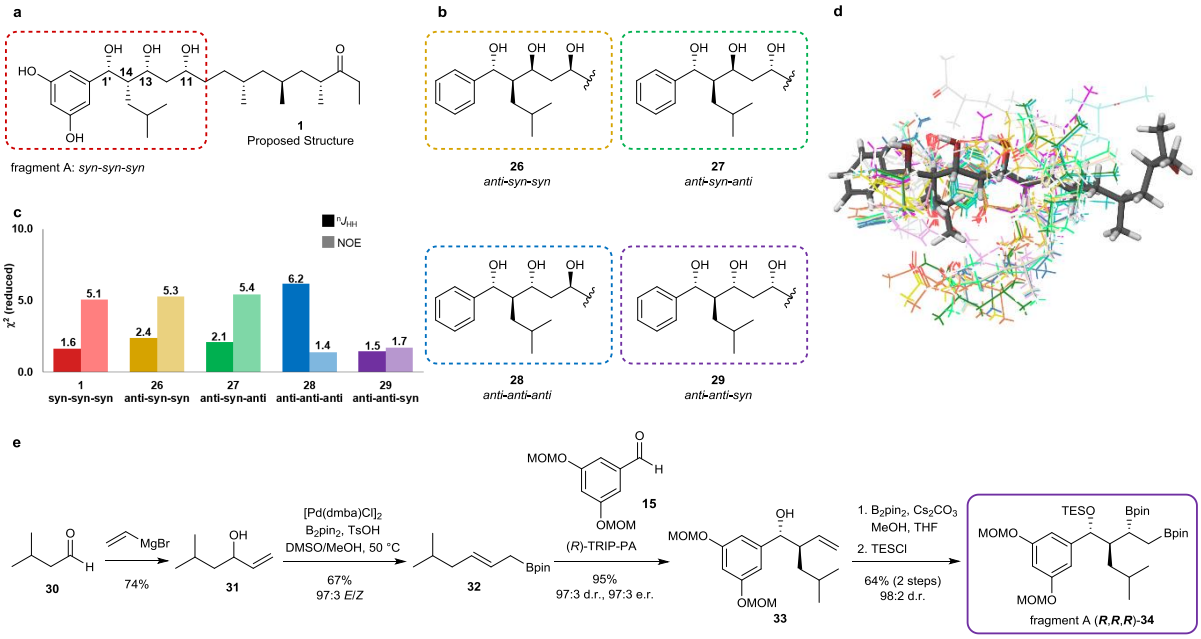

Figure 2. Stereochemical analysis and synthesis of fragment A. a, The proposed structure of baulamycin A (**1**) from Sherman *et al.*[8] highlighting fragment A. **b**, Structures of fragment A diastereomers **26**–**29** used in DFT predictions of NMR parameters for C10–C1′. **c**, Computed C10–C1′ NMR parameters (^{1}H–^{1}H coupling constants, NOE distances) of **26**–**29** and **1** were compared to the corresponding experimental data of the natural product. Diastereomer **29** is the only viable fit (χ^2(reduced) ~1) to the corresponding experimental data. **d**, An overlay of all conformers of **29** analysed with DFT calculations. **e**, Synthesis of revised fragment A (***R***,***R***,***R***)-**34**. [Pd(dmba)Cl]$_2$, di-μ-chlorobis{2-[(dimethylamino)methyl]phenyl-C,N}dipalladium(II).

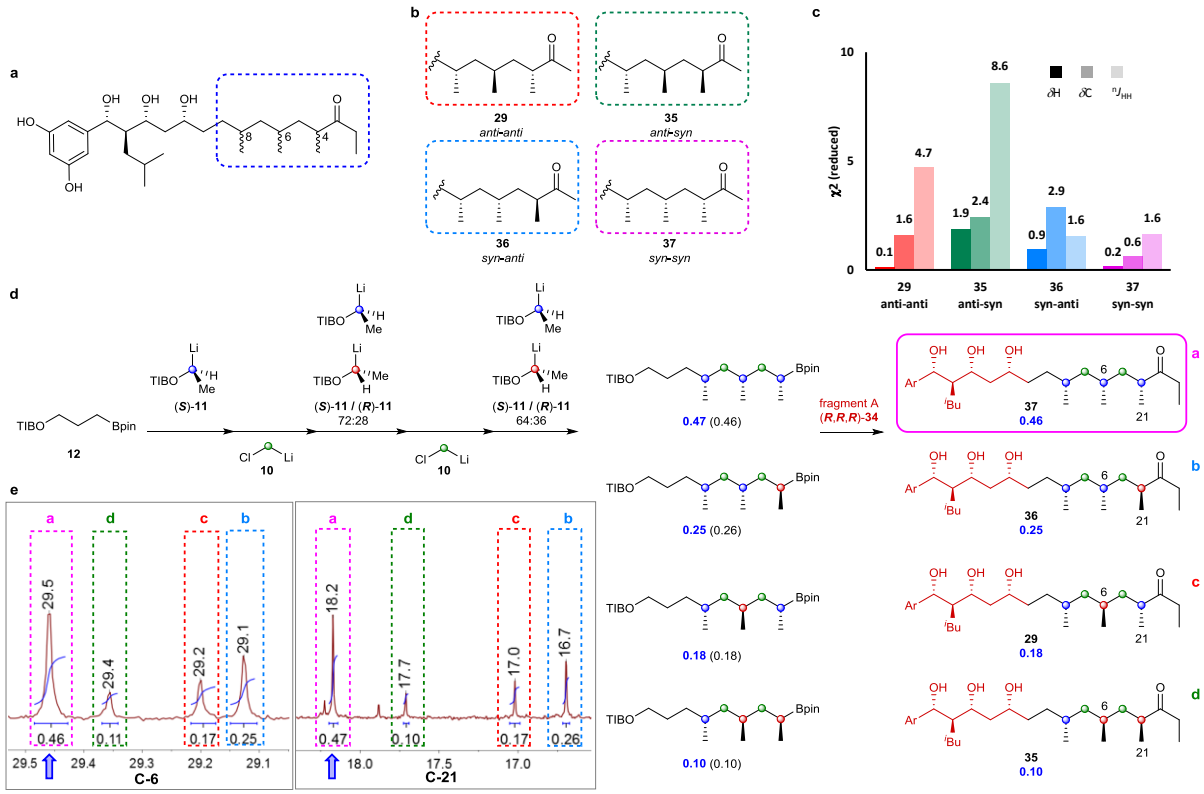

Figure 3. Stereochemical analysis and synthesis of fragment B. **a**, Isomers of baulamycin A based on **29**, highlighting fragment B. **b**, Fragment B diastereomers **29** and **35**–**37**. **c**, Comparison of computed C4–C8 NMR parameters of **29** and **35**–**37** with experimental data. **29** and **35** can be excluded (χ^2(reduced) >>1) and **37** is the most viable fit; **36** may not be confidently excluded. **d**, Synthesis of an encoded mixture of baulamycin A diastereomers (by virtue of known but inequivalent amounts of each isomer). **e**, Comparison of the resulting ^{13}C NMR spectrum (C6 and C21) with that of the natural product indicating a match for signals corresponding to **37** (a).

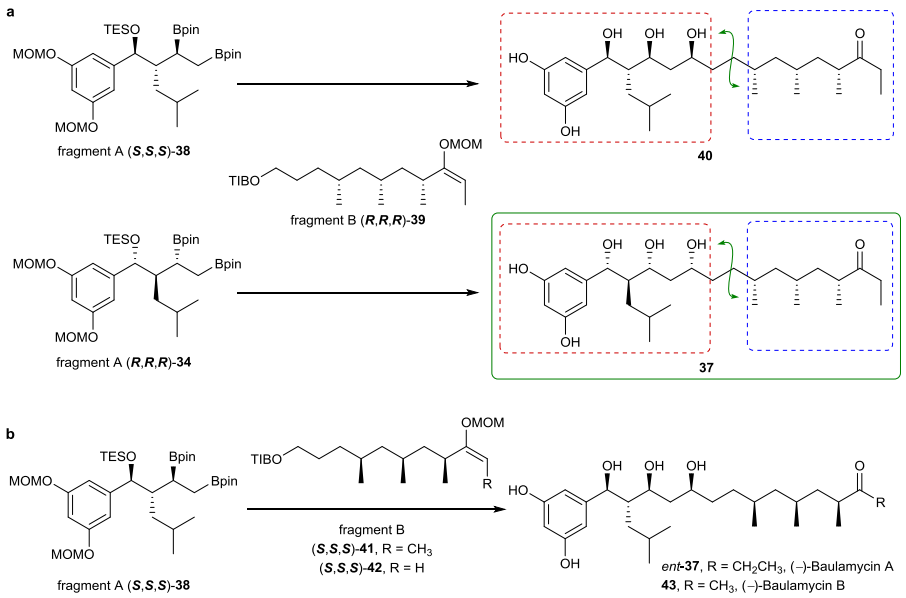

Figure 4. Determination of relative and absolute configuration of baulamycins A and B. **a**, Reaction of the two enantiomers of fragment A (***S***,***S***,***S***)-**38** and (***R***,***R***,***R***)-**34**) with one enantiomer of fragment B ((***R***,***R***,***R***)-**39**). Comparison of the ^{1}H and ^{13}C NMR of compounds **40** and **37** revealed that **37** had the same relative configuration as baulamycin A, but had opposite optical rotation to the natural product. **b**, Coupling of fragments A (***S***,***S***,***S***)-**38** and B ((***S***,***S***,***S***)-**41** and (***S***,***S***,***S***)-**42**) to give the correct structure of baulamycin A (**ent-37**) and B (**43**).